A semi-automatic segmentation method for meningioma developed using a variational approach model

Liam Burrows[1], Jay Patel[2], Abdurrahman I Islim[3,4] , Michael D Jenkinson[5,6], Samantha J Mills[2,6] and Ke Chen[1,7]

Abstract

Background: Meningioma is the commonest primary brain tumour. Volumetric post-contrast magnetic resonance imaging (MRI) is recognised as gold standard for delineation of meningioma volume but is hindered by manual processing times. We aimed to investigate the utility of a model-based variational approach in segmenting meningioma.

Methods: A database of patients with a meningioma (2007–2015) was queried for patients with a contrast-enhanced volumetric MRI, who had consented to a research tissue biobank. Manual segmentation by a neuroradiologist was performed and results were compared to the mathematical model, using a battery of tests including the Sørensen–Dice coefficient (DICE) and JACCARD index. A publicly available meningioma dataset (708 segmented T1 contrast-enhanced slices) was also used to test the reliability of the model.

Results: 49 meningioma cases were included. The most common meningioma location was convexity (n = 15, 30.6%). The mathematical model segmented all but one incidental meningioma, which failed due to the lack of contrast uptake. The median meningioma volume by manual segmentation was 19.0 cm^3 (IQR 4.9–31.2). The median meningioma volume using the mathematical model was 16.9 cm^3 (IQR 4.6–28.34). The mean DICE score was 0.90 (SD = 0.04). The mean JACCARD index was 0.82 (SD = 0.07). For the publicly available dataset, the mean DICE and JACCARD scores were 0.90 (SD = 0.06) and 0.82 (SD = 0.10), respectively.

Conclusions: Segmentation of meningioma volume using the proposed mathematical model was possible with accurate results. Application of this model on contrast-enhanced volumetric imaging may help reduce work burden on neuroradiologists with the increasing number in meningioma diagnoses.

Keywords
Meningioma, monitoring, segmentation

Introduction

Imaging in the management of intracranial meningioma

The extent of imaging follow-up a patient with meningioma receives depends on clinical factors such as neurological symptoms, the histological grade and the elapsed time since initial diagnosis. Follow-up imaging strategies can range from every 3 months for malignant meningioma to every few years for incidental asymptomatic tumours.[1,2] The amount of MRI scanning for intracranial meningioma is increasing.[3] A comprehensive surveillance strategy of meningioma enables patients and clinicians to optimise the timing of any treatment intervention, particularly for incidental meningioma;[4,5] accurate assessment is important when interpreting follow-up MRI for intracranial meningioma as growth can alter management. Additionally, prior studies have suggested that for post-operative patients, tumour volume at follow-up can be more influential at predicting recurrence than extent of resection. Despite this, there is scarce reporting of volumetric rather than two-dimensional measurements.[6]

The slow adoption of volumetric MRI sequences is due to marginally increased acquisition times, increased workload for reporting radiologists and increased incidental findings. The advantages of volumetric studies include increased lesion

[1]Department of Mathematical Sciences and Centre for Mathematical Imaging Techniques, University of Liverpool, UK
[2]Department of Neuroradiology, The Walton Centre NHS Foundation Trust, UK
[3]Geoffrey Jefferson Brain Research Centre, The Manchester Academic Health Science Centre, Northern Care Alliance NHS Group, University of Manchester, UK
[4]Department of Neurosurgery, Manchester Centre for Clinical Neurosciences, Salford Royal Hospital, Northren Care Alliance NHS Foundation Trust, UK
[5]Department of Neurosurgery, The Walton Centre NHS Foundation Trust, UK
[6]Department of Pharmacology and Therapeutics, Institute of Systems, Molecular and Integrative Biology, University of Liverpool, UK
[7]Department of Mathematics and Statistics, University of Strathclyde, UK

Corresponding author:
Abdurrahman I Islim, Geoffrey Jefferson Brain Research Centre, Clinical Sciences Building, Northern Care Alliance NHS Foundation Trust, Salford, M6 8FJ, UK.
Email: Abdurrahman.Islim@manchester.ac.uk

conspicuity (with more accurate delineation of tumour volume) and co-registration techniques to allow direct comparison.[7]

The increasing trend in intracranial meningioma follow-up therefore necessitates adjuncts for the reporting radiologist to improve efficiency and accuracy when determining meningioma growth.

Image segmentation

Image segmentation has been a widely studied topic in the last few decades. Model-based methods, particularly of the variational type, have proven to be effective and robust for a wide range of clinical applications.[8–10] These variational methods use features (such as intensity and texture) directly in the model and output a segmentation result based on certain specified criteria (e.g. the model may encourage the segmentation result to include regions with a high intensity and penalise regions with a low intensity).

In recent years, deep learning methods have become the dominant method of image segmentation.[11–13] Deep learning methods are data driven, requiring a large set of labelled data (data with manual segmentation performed by an expert) in order to train the networks. Typically, convolutional neural networks are given a large database of images as input, and by minimising a loss function, which encourages the output of the network to be similar to the associated ground truth segmentation, the neural network can be trained to perform the task associated with the dataset. A clear disadvantage of the deep learning approach for segmentation is that gathering a labelled dataset large enough to produce good results is time consuming and expensive to do. This motivates the desire to make use of robust variational models which can be unsupervised, and produce results without such large, labelled datasets.

We propose to tackle the problem of meningioma segmentation using a model-based variational approach. Unlike deep learning methods, a variational model is run independently on each image, and so the results can't be influenced by a potential selection bias in the training set. This study will assess the reliability of such a model for meningioma segmentation.

Methods

Patient selection and study design

A retrospectively maintained cohort of patients with an intracranial meningioma was queried for the purpose of this study (January 2007–December 2015). Patients who underwent surgery and consented to the Liverpool Neuroscience Biobank were eligible for inclusion and use of their scans. Further inclusion criteria included the availability of a preoperative volumetric post-contrast MRI. There were no exclusion criteria applied with regards to meningioma location and volume. A post-contrast volume T1-weighted MRI sequence for each patient was processed using manual segmentation, performed by a neuroradiologist, and semi-automatic segmentation, using the proposed mathematical model in this study. As this was a retrospective study, local imaging was acquired on variety of both 1.5T and 3T MRI scanners (parameters for the local scanner acquisitions are

available in Table 1). Additional data collected for each patient included age at time of diagnosis, sex, meningioma location (according to the International Consortium on Meningioma),[14] and meningioma grade and histological sub-type, according to the 2016 World Health Organisation classification system.[15] In addition, a public dataset (https://www.kaggle.com/datasets/awsaf49/brain-tumor), which contains 708 2D T1 contrast-enhanced slices of meningioma, was used to validate the reliability of the proposed variational approach model. The images in the dataset had an inplane resolution of 512×512 with a pixel size of 0.49×0.49 mm^2. The slice thickness was 6 mm with a slice gap is 1 mm. Image quality was to an acceptable diagnostic standard.

Manual segmentation

Manual segmentation for quantitative volumetric measurements of meningioma was undertaken on isotropic 3D T1-weighted post-gadolinium contrast-enhanced studies in the axial plane using ITK-SNAP (https://www.itksnap.org/).[16] Contours were drawn around the target lesion in each slice using the polygon tool and/or the paintbrush tool. The lesions were identified by extra-axial, dural-based mass lesions, most of which demonstrated homogenous enhancement with some internal flow voids due to vascularity. If the meningioma made contact with critical structures, but did not invade or surround the critical structure, segmentation did not include these in the measurement. If there was radiological invasion/involvement, then the enhancing component of the lesion was included in the contours of the segmentation. This applied to vascular structures, such as the superior sagittal, transverse, sigmoid and cavernous sinuses or confluence of dural venous sinuses. If cortical veins made contact with, but were not surrounded by the lesions, then these were not included in the volumetric measurement. Adjacent enhancing dural tails were not included in measurement. Measurement of intraosseous components or adjacent bony hyperostosis was not included. The meningioma in the publicly available dataset were segmented by the primary developer and appropriateness of this segmentation was confirmed by a neuroradiologist.

Mathematical model

The mathematical segmentation method, proposed by Roberts and Spencer,[17] was used to segment meningioma in a semi-automatic fashion. The method requires a user to manually click on the region of interest in a few slices throughout the volume (3–5 clicks). From the user-provided marker points, an edge weighted geodesic distance was calculated. This served as a distance constraint in order to penalise objects away from the region of interest. The marker points also allowed us to initialise the model close to the minimum (though this is not strictly necessary, as the model is globally convex). With the geodesic distance, we ran the variational model to produce a segmentation result. A summary is found in Figure 1, and in the following, we discuss the details mathematically.

$\Omega \subset \mathbb{R}^3$ was denoted as the image domain and a given image as $z : \Omega \to \mathbb{R}$. We used the model in Roberts and Spencer,[17] which first involved calculating the geodesic distance.[18] A set of k marker points was defined by

Table 1. Parameters for the scanner acquisitions.

Scanner	Field strength(T)	Sequence	TR (ms)	TE (ms)	TIR (ms)	Slice thickness(mm)	Slice gap
GE	3.0	FSPGR	8.132	3.164	450	1.4	no gap
Philips	3.0	SENSE	9	1.366	n/a	1	no gap
GE	1.5	FSPGR	10.516	4.208	450	1.4	no gap
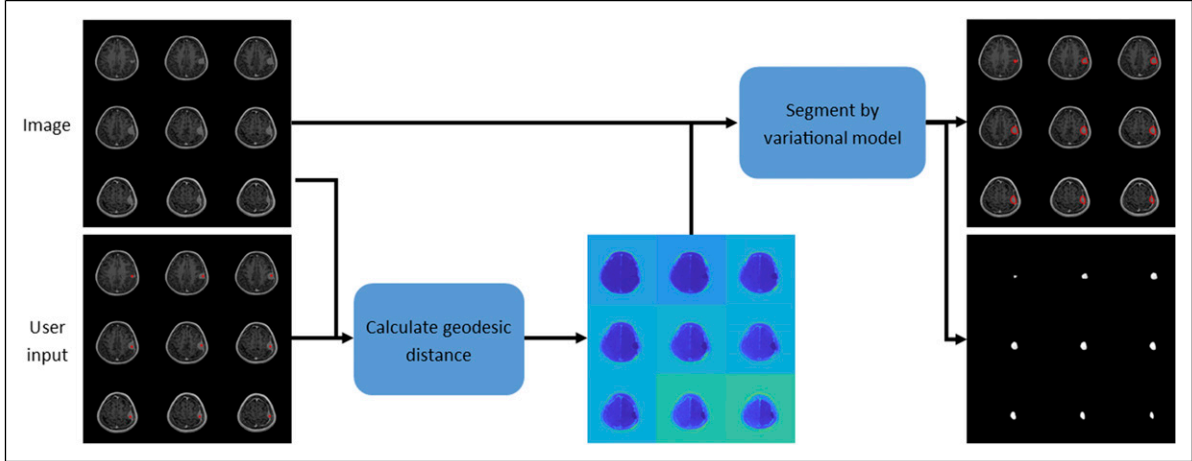
Figure 1. A schematic representation of the model-based variational approach to meningioma segmentation.

$\mathcal{M} = \{\mathbf{x}_i \in \Omega : 1 \leq i \leq k\}$, indicating the position of the region of interest. In this method, we only required $3 - 4$ clicks in the whole volume, that is, $k \leq 4$. Our method belonged to the class of local and selective segmentation models that aimed to segment one region of interest only. To calculate the geodesic distance, we solved the Eikonal equation:

$$\begin{cases} |\nabla \mathcal{D}_0(\mathbf{x})| = \epsilon + \beta|\nabla z(\mathbf{x})|^2, & \mathbf{x} \in \Omega \\ \mathcal{D}_0(\mathbf{x}) = 0, & \mathbf{x} \in \mathcal{M}, \end{cases}$$

with the final geodesic distance being: $\mathcal{D}(\mathbf{x}) = \frac{\mathcal{D}_0(\mathbf{x})}{\|\mathcal{D}_0(\mathbf{x})\|_{L^\infty}}$.

With the Eikonal equation solved, we achieved segmentation by minimising the following energy:

$$E(u) = \int_\Omega g(|\nabla z|)|\nabla u|\,d\mathbf{x} + \lambda \int_\Omega (f_1(z) - f_2(z))u\,d + \theta \int_\Omega \mathcal{D}u\,d\mathbf{x},$$

where $g(s) = \frac{1}{1+\iota s^2}$ is an edge detector, $f_1(z) = (z - c_1)^2$, and

$$f_2(z) = \begin{cases} 1 + \dfrac{z - c_1}{\gamma_1}, & c_1 - \gamma_1 \leq z \leq c_1, \\ 1 - \dfrac{z - c_1}{\gamma_2}, & c_1 \leq z \leq c_1 + \gamma_2, \\ 0, & \text{else}, \end{cases}$$

where γ_1 and γ_2 are defined as in Roberts and Spencer.[17] The final segmentation result was denoted as the set $\Sigma = \{\mathbf{x} \in \Omega : u(\mathbf{x}) > 0.5\}$.

Statistical analysis

Data are presented as number (%), median (interquartile range [IQR]) or mean (standard deviation [SD]) as appropriate. The segmentation results were compared using standard metrics including the Sørensen–Dice coefficient (DICE), JACCARD index, volumetric similarity (VS) coefficient and Haussdorff distance (HD).[19] Both DICE and JACCARD scores range between 0 (where no overlap between compared segmentation results occurs) and 1 (where the two segmentation results are an exact match). VS represents how similar the volumes of the segmented outputs are, not influenced by the overlap. This also ranges from 0 to 1, the latter being an identical volumetric match. HD describes the largest distance from one volume to the nearest point in the other. The ideal result of HD is a score of 0, as the voxels of the two segmentation results would be in the same place. Bland–Altman plots were constructed to visualise the differences between the volumetric measurements.
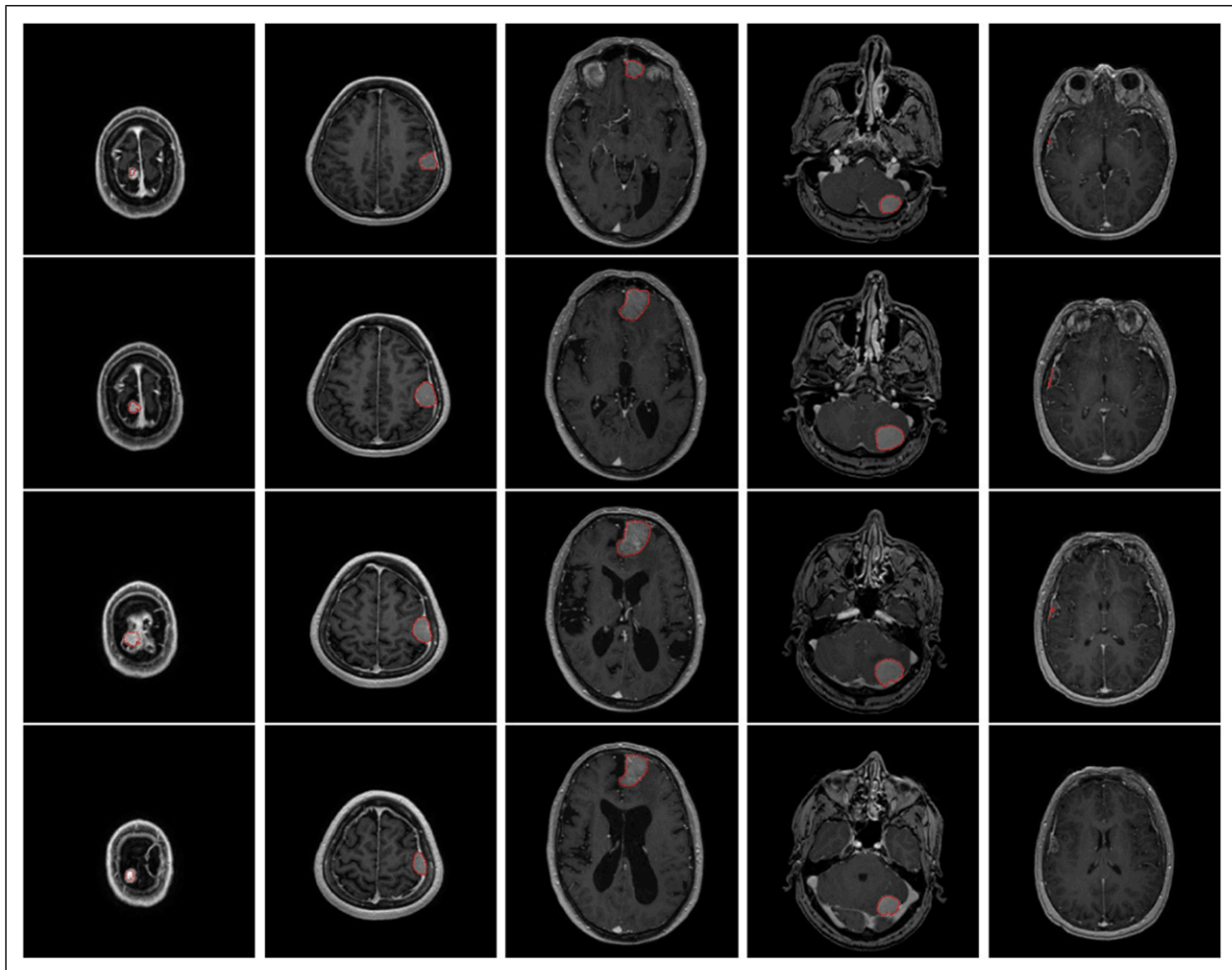
Results

Study participants

Forty-nine patients were included. Their median age at diagnosis was 54 years (IQR 45–62). Forty-one were female (83.7%). All patients had a solitary meningioma in the following locations: convexity ($n = 15$, 30.6%), sphenoid wing ($n = 9$, 18.4%), anterior midline ($n = 9$, 18.4%), posterior fossa - lateral and posterior ($n = 6$, 12.2%), parafalcine ($n = 5$, 10.2%), parasagittal ($n = 3$, 6.1%) and tentorial ($n = 2$, 4.1%). Forty-four meningioma were WHO grade 1 (89.8%) and 5 were WHO grade 2 (10.2%). Patient details are summarised in Table 2.

Volume calculations

All but one tumour could be segmented using the mathematical model. A patient with a convexity meningioma (case 5, Figure 2) could not have their meningioma segmented due

Table 2. Characteristics of the 49 patients included in the study.

Age (median, IQR)		54 (45−62)
Sex (*N*, %)	Female	41 (83.7)
	Male	8 (16.3)
Meningioma location (*N*, %)	Convexity	15 (30.6)
	Sphenoid wing	9 (18.4)
	Anterior midline	9 (18.4)
	Posterior fossa − lateral and posterior	6 (12.2)
	Parafalcine	5 (10.2)
	Parasagittal	3 (6.1)
	Tentorial	2 (4.1)
WHO grade (*N*, %)	1	44 (89.8)
	2	5 (10.2)
Histopathological subtype (*N*, %)	Meningothelial	17 (34.7)
	Fibrous	7 (14.3)
	Transitional	6 (12.2)
	Psammomatous	5 (10.2)
	Atypical	5 (10.2)
	Angiomatous	2 (10.2)
	Lymphaplasmacyte-rich	1 (2)
	Microcytic	1 (2)
	Secretory	1 (2)
	Not specified	4 (8.2)

Figure 2. Examples of 5 meningioma from the first dataset with their segmentation results using the mathematical model. Each panel represents a meningioma. The meningioma in the last panel could not be segmented due to the lack of contrast uptake.

to lack of uptake of contrast by the tumour. For the remaining cases, the median meningioma volume by manual segmentation was 19.0 cm^3 (IQR 4.9–31.2). The median meningioma volume using the mathematical model was 16.9 cm^3 (IQR 4.6–28.4).

Segmentation comparisons

The mean DICE and JACCARD scores were 0.90 (SD = 0.04) and 0.82 (SD = 0.07), respectively. The mean VS was 0.94 (SD = 0.04). The mean HD was 11.4 (SD = 23.6). The Bland–Altman plot (Figure 3) demonstrates the spread of differences in meningioma volumes. For 46 cases, the difference was between the 95% confidence interval (CI) (−7.6 to 3). Three cases fell outside of the 95% CI. Only 2D slices were available for the public dataset; therefore, volumetric calculations were not possible. However, mean DICE, JACCARD and HD scores were 0.90 (SD = 0.06), 0.82 (SD = 0.10) and 6.08 (SD = 4.6), respectively. The time taken to manually segment a meningioma by a neuroradiologist ranged from 5 to 15 min. The segmentation by the mathematical model required 3–5 clicks in different slices throughout the meningioma volume. This was performed in less than a minute across all cases.

Discussion

In this study, we have demonstrated the use of a robust variational model for meningioma segmentation. The variational model presents several advantages over manual segmentation: namely, the computation time and the time taken for the user to interact with the algorithm. The variational model only needs two to four user clicks throughout a handful of slices in the image, whereas the manual model requires careful supervision by a user throughout the process. We have demonstrated that the variational model can produce an output which is as similar in segmentation and volume measurement to manual segmentation proving that clinically relevant information can be drawn from the variational model

to be used in practice in a more efficient manner. To the authors' knowledge, this mathematical segmentation model has not been used for meningioma segmentation on imaging previously.

Comparison to other segmentation models

Comparison of meningioma segmentation algorithms is challenging as there is no common public database with an established evaluation metric available. The widely used Multimodal Brain Tumor Segmentation Challenge dataset,[20] though stimulating many works in brain tumour segmentation, contains only gliomas and not meningiomas.

Early work segmenting brain tumours include the work by Kaus et al.,[21] who segmented the region of interest on spoiled gradient recalled images by using atlas-based methods and registration, followed by simple operations such as morphological operations and region growing methods as postprocessing. The algorithm developed was based mainly on glioma (6 meningioma and 14 glioma patients), making it less applicable to patients with meningioma. Another work by Hsieh et al. used both T1 and T2-weighted MR images to segment the meningioma region automatically,[22] using fuzzy c-means clustering, followed by region growing and morphological operation (dilation and erosion) to refine the border of the tumour. Their method produces satisfactory results on simple images but struggled where noticeable edema was present. This was likely due to the need for T2-weighted imaging which is more sensitive for detection of edema and therefore may have confounded accurate contouring of the tumour. Our method required T1 imaging only, and therefore, we did not observe this to be an issue.

Variational approaches have also been considered in the literature. The variational approach by Urien et al. is based on the convex relaxed version of the Chan–Vese model.[23,24] The segmentation model assumes 4-phases, performed on contrast-enhanced T1-weighted MR images. In addition, the model itself contains a spatially adaptive parameter which depends on a corresponding positron emission tomography
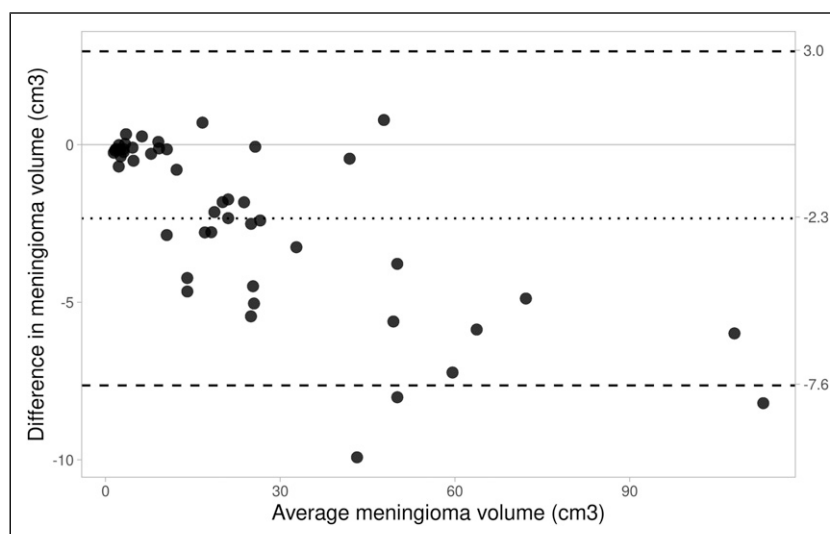
Figure 3. A Bland−Altman plot representing the difference in meningioma volumes by the two segmentation methods. The dotted line represents the average difference in meningioma volume. The dashed lines represent the 95% confidence intervals.

(PET) scan. The motivation behind including a PET scan was that the higher the intensity value of a pixel in the PET, the more likely that pixel is tumour, and thus, using this information in the segmentation model on the T1 image can supplement and aid the segmentation of the meningioma. Despite this, the authors quoted a relatively low accuracy score. Moreover, PET scanning is not routinely performed for meningioma patients, adding doubt to the applicability of this in clinical practice.

In recent years, deep learning techniques have been generally more popular. One such set of work is by Laukamp et al.,[25,26] who used the DeepMedic network architecture using a multimodal dataset (T1, T1 with contrast, T2 and FLAIR) including 126 meningioma patients. Satisfactory results were produced; however, a large amount of pre-processing is necessary, such as atlas registration and skull stripping, which were not features of the model utilised in this study.

Bouget et al. proposed a deep learning method using standard network architectures and simple preprocessing tricks to speed performance up on a large dataset containing 698 contrast-enhanced T1-weighted MRI volumes.[27] In follow-up work,[28] they use the same dataset utilising attention gated mechanisms on top of standard U-Net architectures. They quote an average DICE score of 0.82 and claim a near perfect detection of meningioma greater than 3 cm^3. For meningioma smaller than 3 cm^3, their method is susceptible to failing to detect them. This is likely the result of a bias in the training set (lack of small meningiomas in the data), as well as limitations in the number of voxels to compute features from in the network. Conversely, we did not observe a performance bias towards smaller or larger tumours in our model.

Another recent work by Chen et al. uses a U-Net like architecture to segment tumour images,[29] but also uses a further network to assign a grade to each tumour. A DICE score of 0.87 is quoted for the 3D network on 18 low grade meningioma, proving to be an effective method. However, the authors note that their model failed to segment the tumour section where: the tumour was adjacent to the thickening of the dura mater, located in the anterior skull base, or had certain high-grade meningioma features such as necrosis. The number of each case fulfilling these criteria were not provided and so the number of patients with a successful segmentation could not be estimated. Like the limitations in the study by Bouget et al., these were likely due to a lack of training data for these particular cases, demonstrating a flaw of the deep learning approaches.

Clinical utility, study limitations and future work

Active monitoring of an incidental meningioma is the recommended management choice.[1] Sustained growth is the most common indication for intervention in these cases.[2] The National Cancer Institute recommends the use of volumetric imaging to monitor tumours like meningioma;[7] however, this is limited by the time taken to perform manual segmentation by neuroradiologists. The variational model employed in this study demonstrated accurate delineation of meningioma volume. There were several limitations. Firstly, the study sample size was relatively small; however,

it included a variety of meningioma locations and volumes. Secondly, one patient (4.5%) had a microcystic meningioma, and these do not take up gadolinium contrast, which limited the use of the model. Cystic changes or necrosis within a meningioma impede contrast uptake, and occurs in approximately 10% of patients.[30] For these cases, it may be that segmentation improves with the use of distance constraints inputting 'antimarkers' – clicks which the user inputs to indicate the background, and selecting more tumour areas within the slides. Additionally, the fidelity term in such models dictates which pixel intensity to segment. The fidelity in the used model looked for a particular intensity (based on the user input) and segmented similarly coloured pixels. By developing a new fidelity term, for inhomogeneous regions of interest, the model could be adjusted to consider average pixel intensity in a small neighbourhood around each pixel individually, which is more sophisticated. Third, despite validating the model in a large publicly available dataset, the metrics that could be examined revolved around overlap (DICE and JACCARD) and not volumetric similarity; the reason being availability of 2D slices only. Validation, of both overlap and volumetric metrics, in a larger dataset is required.

Conclusion

Meningioma segmentation using a model-based variational approach is possible with accurate results. Results on meningioma show successful segmentation in most cases.

ORCID iD

Abdurrahman I Islim ⬤ https://orcid.org/0000-0001-9621-043X

References

1. Goldbrunner R, Stavrinou P, Jenkinson MD, et al. EANO guideline on the diagnosis and management of meningiomas. *Neuro Oncol* 2021; 23(11): 1821–1834. DOI: 10.1093/neuonc/noab150.
2. Islim AI, Mohan M, Moon RDC, et al. Incidental intracranial meningiomas: a systematic review and meta-analysis of prognostic factors and outcomes. *J Neuro Oncol* 2019; 142(2): 211–221. DOI: 10.1007/s11060-019-03104-3.
3. Agarwal V, McCutcheon BA, Hughes JD, et al. Trends in management of intracranial meningiomas: analysis of 49,921 cases from modern cohort. *World Neurosurg* 2017; 106: 145–151. DOI: 10.1016/j.wneu.2017.06.127.
4. Lee EJ, Kim JH, Park ES, et al. A novel weighted scoring system for estimating the risk of rapid growth in untreated intracranial meningiomas. *J Neurosurg* 2017; 127(5): 971–980. DOI: 10.3171/2016.9.JNS161669.
5. Islim AI, Kolamunnage-Dona R, Mohan M, et al. A prognostic model to personalize monitoring regimes for patients with

incidental asymptomatic meningiomas. *Neuro Oncol* 2020; 22(2): 278–289. DOI: 10.1093/neuonc/noz160.

6. Gillespie CS, Taweel BA, Richardson GE, et al. Volumetric growth of residual meningioma – a systematic review. *J Clin Neurosci* 2021; 91: 110–117. DOI: 10.1016/j.jocn.2021.06.033.

7. Mills SJ, Radon MR, Baird RD, et al. Utilization of volumetric magnetic resonance imaging for baseline and surveillance imaging in Neuro-oncology. *Br J Radiol* 2019; 92(1098): 20190059. DOI: 10.1259/bjr.20190059.

8. Burrows L, Guo W, Chen K, et al. Reproducible kernel Hilbert space based global and local image segmentation. *Inverse Probl Imag* 2021; 15(1): 1. DOI: 10.3934/ipi.2020048.

9. Zhao Y, Rada L, Chen K, et al. Automated vessel segmentation using infinite perimeter active contour model with hybrid region information with application to retinal images. *IEEE Trans Med Imag* 2015; 34(9): 1797–1807. DOI: 10.1109/TMI.2015.2409024.

10. Zohios C, Kossioris G and Papaharilaou Y. Geometrical methods for level set based abdominal aortic aneurysm thrombus and outer wall 2D image segmentation. *Comput Methods Progr Biomed* 2012; 107(2): 202–217. DOI: 10.1016/j.cmpb.2011.06.009.

11. Chen LC, Papandreou G, Kokkinos I, et al. DeepLab: semantic image segmentation with deep convolutional nets, atrous convolution, and fully connected CRFs. *IEEE Trans Pattern Anal Mach Intell* 2018; 40(4): 834–848. DOI: 10.1109/TPAMI.2017.2699184.

12. Chen LC, Papandreou G, Schroff F, et al. *Rethinking atrous convolution for semantic image segmentation*. arXiv, 2017.

13. Ronneberger O, Fischer P and Brox T. U-net: convolutional networks for biomedical image segmentation. In: Navab N, Hornegger J, Wells WM, et al. (eds). *Medical Image Computing and Computer-Assisted Intervention – MICCAI 2015. Lecture Notes in Computer Science*. Berlin: Springer International Publishing, 2015: 234–241. DOI: 10.1007/978-3-319-24574-4_28.

14. Nassiri F, Wang JZ, Au K, et al. Consensus core clinical data elements for meningiomas (v2021.1). *Neuro Oncol* 2022; 24(5): 683–693. DOI: 10.1093/neuonc/noab259.

15. Louis DN, Perry A, Reifenberger G, et al. The 2016 World Health organization classification of tumors of the central nervous system: a summary. *Acta Neuropathol* 2016; 131(6): 803–820. DOI: 10.1007/s00401-016-1545-1.

16. Yushkevich PA, Piven J, Hazlett HC, et al. User-guided 3D active contour segmentation of anatomical structures: significantly improved efficiency and reliability. *Neuroimage* 2006; 31(3): 1116–1128. DOI: 10.1016/j.neuroimage.2006.01.015.

17. Roberts M and Spencer J. Chan–Vese reformulation for selective image segmentation. *J Math Imag Vis* 2019; 61(8): 1173–1196. DOI: 10.1007/s10851-019-00893-0.

18. Roberts M, Chen K and Irion KL. A convex geodesic selective model for image segmentation. *J Math Imag Vis* 2019; 61(4): 482–503. DOI: 10.1007/s10851-018-0857-2.

19. Burrows L, Chen K, Guo W, et al. Evaluation of a hybrid pipeline for automated segmentation of solid lesions based on mathematical algorithms and deep learning. *Sci Rep* 2022; 12(1): 14216. DOI: 10.1038/s41598-022-18173-0.

20. Menze BH, Jakab A, Bauer S, et al. The multimodal brain tumor image segmentation benchmark (BRATS). *IEEE Trans Med Imag* 2015; 34(10): 1993–2024. DOI: 10.1109/TMI.2014.2377694.

21. Kaus MR, Warfield SK, Nabavi A, et al. Automated segmentation of MR images of brain tumors. *Radiology* 2001; 218(2): 586–591. DOI: 10.1148/radiology.218.2.r01fe44586.

22. Hsieh TM, Liu YM, Liao CC, et al. Automatic segmentation of meningioma from non-contrasted brain MRI integrating fuzzy clustering and region growing. *BMC Med Inf Decis Making* 2011; 11(1): 54. DOI: 10.1186/1472-6947-11-54.

23. Urien H, Buvat I, Rougon N, et al. 3D PET-driven multi-phase segmentation of meningiomas in MRI. In: 2016 IEEE 13th international symposium on biomedical imaging (ISBI). 13-16 April 2016. Prague, Czech Republic: 407–410. DOI: 10.1109/ISBI.2016.7493294

24. Chan TF, Esedoglu S and Nikolova M. Algorithms for finding global minimizers of image segmentation and denoising models. *SIAM J Appl Math* 2006; 66(5): 1632–1648. DOI: 10.1137/040615286.

25. Laukamp KR, Pennig L, Thiele F, et al. Automated meningioma segmentation in multiparametric MRI. *Clin Neuroradiol* 2021; 31(2): 357–366. DOI: 10.1007/s00062-020-00884-4.

26. Laukamp KR, Thiele F, Shakirin G, et al. Fully automated detection and segmentation of meningiomas using deep learning on routine multiparametric MRI. *Eur Radiol* 2019; 29(1): 124–132. DOI: 10.1007/s00330-018-5595-8.

27. Bouget D, Pedersen A, Hosainey SAM, et al. Fast meningioma segmentation in T1-weighted magnetic resonance imaging volumes using a lightweight 3D deep learning architecture. *J Med Imaging* 2021; 8(2): 024002. DOI: 10.1117/1.JMI.8.2.024002.

28. Bouget D, Pedersen A, Hosainey SAM, et al. Meningioma segmentation in T1-weighted MRI leveraging global context and attention mechanisms. *Front Radiol* 2021: 1, https://www.frontiersin.org/articles/10.3389/fradi.2021.711514 (Accessed 19 October 2022).

29. Chen C, Cheng Y, Xu J, et al. Automatic meningioma segmentation and grading prediction: a hybrid deep-learning method. *J Personalized Med* 2021; 11(8): 786. DOI: 10.3390/jpm11080786.

30. Morin O, Chen WC, Nassiri F, et al. Integrated models incorporating radiologic and radiomic features predict meningioma grade, local failure, and overall survival. *Neuro-Oncol Adv* 2019; 1(1): vdz011. DOI: 10.1093/noajnl/vdz011.